Palmer

DOE/ER/83060

PHASE I – FINAL REPORT

Improved Position Sensitive Detectors for Thermal Neutrons

U. S. Department of Energy
Small Business Innovative Research Grant

DE-FG02-00ER83060

Phase I, Oct. 2000 – March 2001

Design, Fabrication, and Results of Testing the Phase I - Proof-of-Principal Improved Position Sensitive Thermal Neutron Detector Prototype in the Laboratory and at the Intense Pulsed Neutron Source (IPNS), Argonne National Laboratory

Dr. Carter Hull, Principal Investigator

Nuclear Safeguards and Security Systems, LLC
11020 Solway School Road
Knoxville (Oak Ridge), TN 37931

(865) 927-9999

http://www.nucsafe.com/

DISCLAIMER

IMPROVED POSITION SENSITIVE DETECTORS FOR THERMAL NEUTRONS

BACKGROUND, GOALS AND COMPLETED RESEARCH

Nuclear Safeguards and Security Systems, LLC (NucSafe) of Oak Ridge, Tennessee was awarded a Phase I SBIR Grant to develop Improved Position Sensitive Detectors for Thermal Neutrons. The primary goals of Phase I and II research are to design, test, and determine the technical feasibility of developing two-dimensional (2D) position sensitive, scintillating glass Fiber Detectors (FD) for neutron scattering research centers, particularly large area detectors for the SNS. This document is a synopsis of Phase I research, results and discussion of testing the prototype FD, and conclusions drawn from this work.

Neutron glass fibers are not as susceptible to gamma interactions as scintillator plates and wave-guides are not required since the fibers themselves act as the wave-guides and are used to provide neutron capture positioning data. Not many strands of neutron glass fiber are necessary to make thin fiber ribbons. Each ribbon can be electronically independent for timing and throughput as one of many detector elements in a high resolution array. The total time for individual neutron captures, fluorescence and "relaxation," and all signal processing is typically less than ~400 nanoseconds (ns). This fast reaction and processing time, combined with the glass fiber detector medium that is relatively inexpensive and flexible, are attractive attributes for developing position sensitive detector arrays. Electronics developed by NucSafe for neutron glass fiber detectors utilize pulse height analysis discrimination and very fast coincidence circuitry, which allows very high neutron – gamma discrimination ratios. Through pulse-height discrimination alone, neutron to gamma discrimination ratios of >8500:1 have been achieved in thick glass fiber bundles. Ratios as high as 60,000:1 may be achievable with new fast electronic circuitry that is currently being tested.

The Phase I proof-of-principal detector was conceptualized and designed to be position sensitive in 1D and then be expanded to test for 2D position sensitivity in Phase II. The Phase I work plan and deliverables were to design, fabricate and test a neutron detector prototype that utilizes neutron glass fibers as detector elements. These single, or at most double, fiber layers were initially planned to be configured into parallel strips of 1 mm in width or less with fiber lengths of 50 cm of so in the prototype detector. A number of these fiber strips arranged parallel to one another constitutes a 1D detector with a resolution somewhat less than the width of the strip; *i.e.*, 1 mm or so in the prototype.

This was the basic proposition and goal of Phase I R&D – to find out how the glass fibers respond to scattered neutrons and perhaps incident beams in pulsed neutron environments and in high flux reactor environments. The proof-of-principal prototype also was to test neutron-gamma sensitivity and that neutron-gamma discrimination for neutron glass fibers is suitable in both pulsed and steady state neutron source environments. In fact, a much more extensive proof-of-principal prototype detector was fabricated, which delivers significantly more that proposed in the Phase I research plan. The detector platform was expanded to allow for testing of not only 1D position sensitivity, but also 2D for populations of neutron captures. The prototype detector was designed so that is was useful for Phase I and could then be scaled up for the initial portions of Phase II R&D. Phase II will focus on 2D position sensitivity for individual neutron interactions using a minimum of two "crossed-fiber" designs for 2D position sensitivity.

Research Completed in Phase I

Proof-of-Principal Fiber Detector for Thermal Neutron Detection and Discrimination

The proof-of-principal position sensitive fiber detector is quite different than the large panels that are developed by NucSafe (the Small Business Concern) for passively detecting and measuring thermalized neutrons at very low count rates. NucSafe has extensively tested large area neutron glass fiber panels for over two years during the IAEA ITRAP evaluation of detector systems for nuclear non-proliferation and illegal trafficking of nuclear materials (Hull, 2001a).

Goals for the prototype Fiber Detector (FD) were to gather data and properly discriminate neutron and gamma signals in real time. The Phase I system was designed to be position sensitive in one dimension (1D) and have the capability of 2D measurements in Phase II. The Phase II system is planned to have high throughput and saturation levels while detecting and recording individual neutron arrivals in 2D with very fast detection and signal processing times.

The concept for the NucSafe Phase I FD is somewhat similar to the cross-fiber detectors scintillation systems constructed by Wright, Hutchinson, Richards, and Holcomb (1998). These prototypes, and to an extent their wand detectors, are analogous to the proposed FD in that scintillation is the medium and optoelectronics are utilized to detector and "plot" the loci of the neutron interactions. However, no scintillator plate is used in the glass fiber detector – the scintillation plate and the wave shifting guides are replaced by the fibers.

- Design and Fabrication of the Prototype Position Sensitive Fiber Detector

  - MCNP models were run to get initial feelings for the detection quantum efficiency in various configurations prior to finalizing a preliminary Fiber Detector design.

  - Neutron sensitive glass fibers were to be arranged in thin strips of double layers of fibers – these are referred to as bilayers. About 7 adjacent glass fibers with cladding arranged in a single layer are about 1 mm in width. Thin fiber strips were configured as adjacent ribbons 0.5 cm in width (the resolution dimension that was chosen to be tested). Fiber lengths were dictated by the sample well used for testing at IPNS.

  - Each fiber ribbon was coupled at each end so coincidence circuitry was applied as well as pulse height analysis to discriminate gamma and neutron signals.

  - Processing electronics can now handle 1 MHz with very little dead time and fluorescence and processing times allow count rates to ~10^8 *per* channel using the current electronics.

The modeling of 0.50 cm wide X and Y neutron glass fiber ribbons indicated that one, at most two, bilayers are required for the neutron energies at IPNS. One glass fiber "bilayer" is simply two layers of fibers like in the "end-on" view shown in **Figure 1** below:

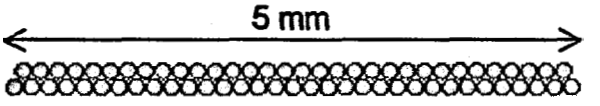

Figure 1. Neutron glass fiber bilayer – end-on view. Individual fiber diameters are 100 μm. The silicone cladding on individual fibers results in packing diameters of ~150 mm.

A "cartoon" of the final prototype design is shown in **Figure 2**. The "X" and "Y" fiber ribbons that comprise the detector "elements" are shown in orange and blue in the figure. This diagram shows only the detector base plate, ribbon channels occupied with neutron fiber ribbons and passive wave shifting fibers, photomultiplier tubes, and general configuration. The prototype detector as deployed in its light-tight casing is not depicted. The objectives for testing this prototype in the laboratory and in the "field" at IPNS were to: detect scattered neutrons from a pulsed source, determine if neutron glass fibers are useful as detectors in this environment, find out if the system can clearly discriminate neutron from gamma events, get an idea of the best electronic configurations for measurements, determine the position sensitivity and throughput for the detector ribbons, and use these tests to evaluate scaling up the prototype.

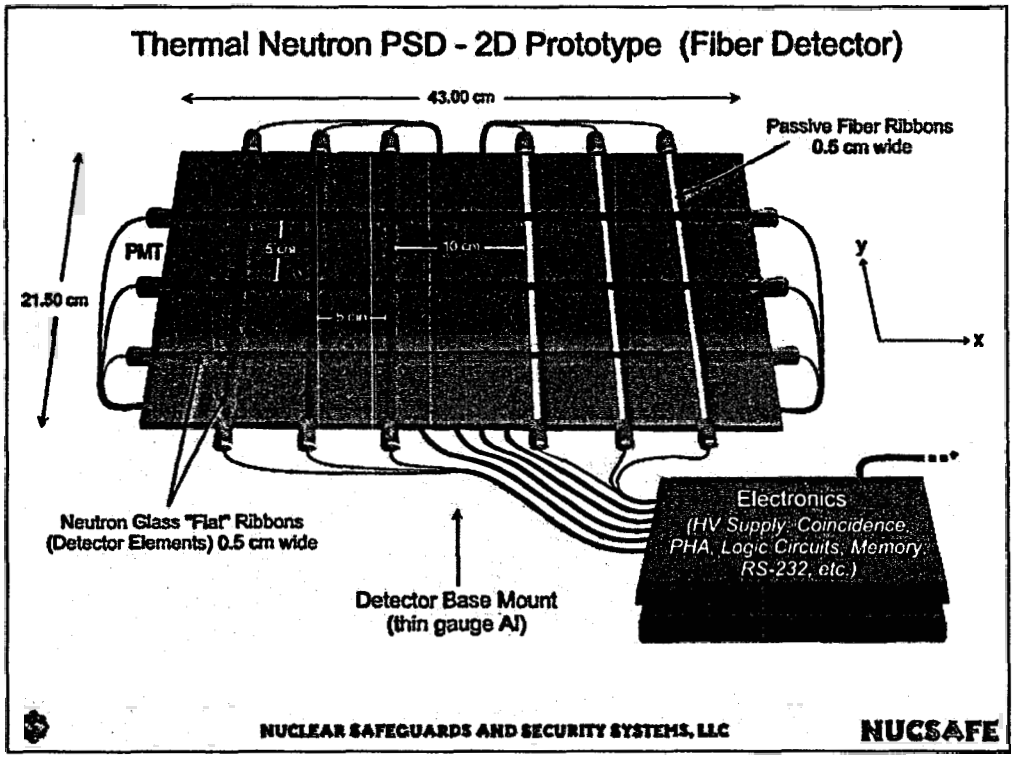

Figure 2. Simplified diagram of the prototype position sensitive neutron detector developed during Phase I SBIR research.

The technical specifications for the prototype detector (particularly the base plate) are shown more clearly in the mechanical drawings included as **Figures 3** and **4**. The overall

dimensions of the detector are based upon the volume of the sample well in the testing area to be used at IPNS (QUIP). The relatively large 5 cm spacings between the ribbons (spacings are 10 times that of a fiber ribbon width) were designed to allow the individual ribbons to be isolated by "masking" off detector element ribbons by constructing neutron masks around specific areas of the X-Y fiber ribbons and ribbon intersection "nodes." The large intervals were chosen in order to minimize neutron interactions except with the area being measured for position sensitivity.

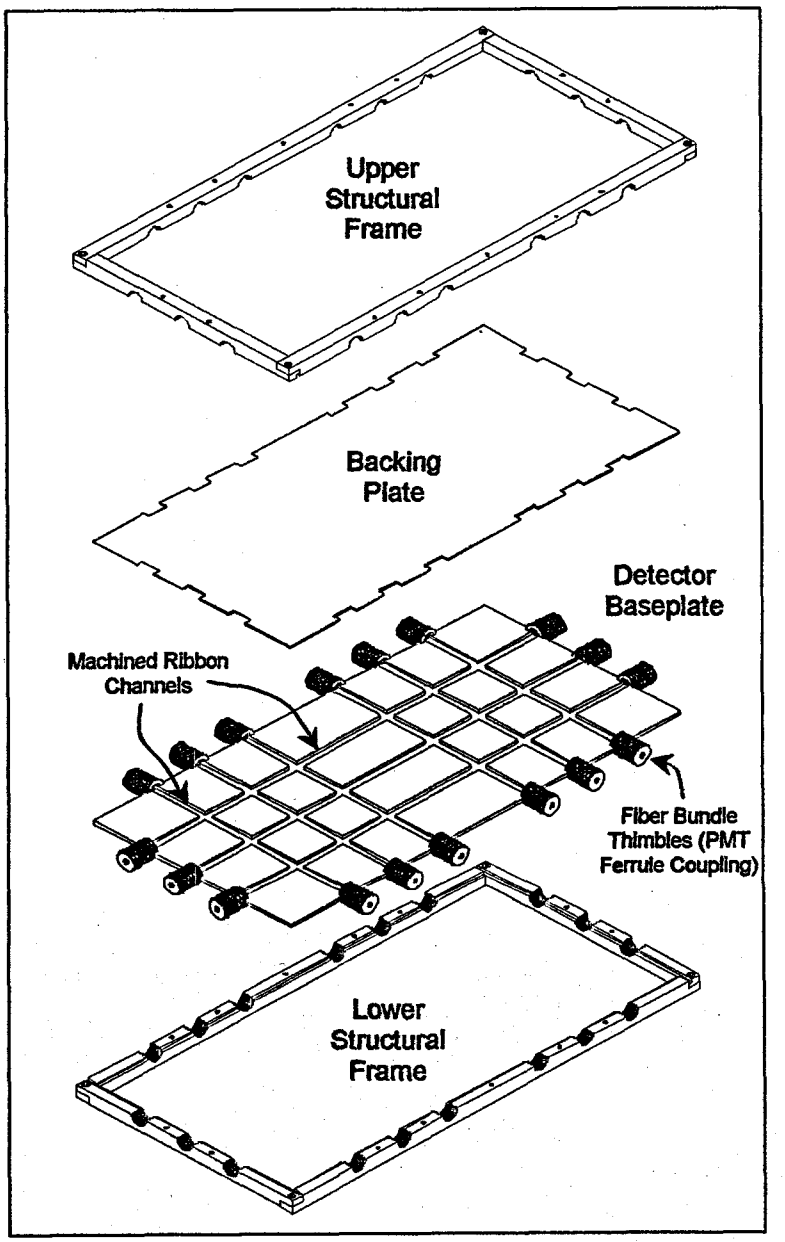

Figure 3. CAD diagram of the Phase I prototype position sensitive neutron detector (light tight enclosure is not shown). The square spacings on the detector baseplate between X and Y neutron glass fiber ribbon elements are 5 cm. The prototype detector has two "halves" as described in the text.

The prototype detector baseplate was designed for housing two types of crossed fiber detectors. Each detector "half" is planned to be tested separately; the first during in Phase I and the second during the early part of Phase II. This concept was used to minimize re-design and engineering costs if the initial tests warranted ongoing development of the detector systems. This may be explained more easily by use of the diagram shown in **Figure 4**, a mechanical drawing to scale of the detector baseplate with specifications (unfortunately, still in English measurement units). The baseplate was machined from very high purity aluminum to minimize activation products. The parallel lines at right angles are the channels that were machined into the baseplate to contain the fiber ribbons in the desired geometries.

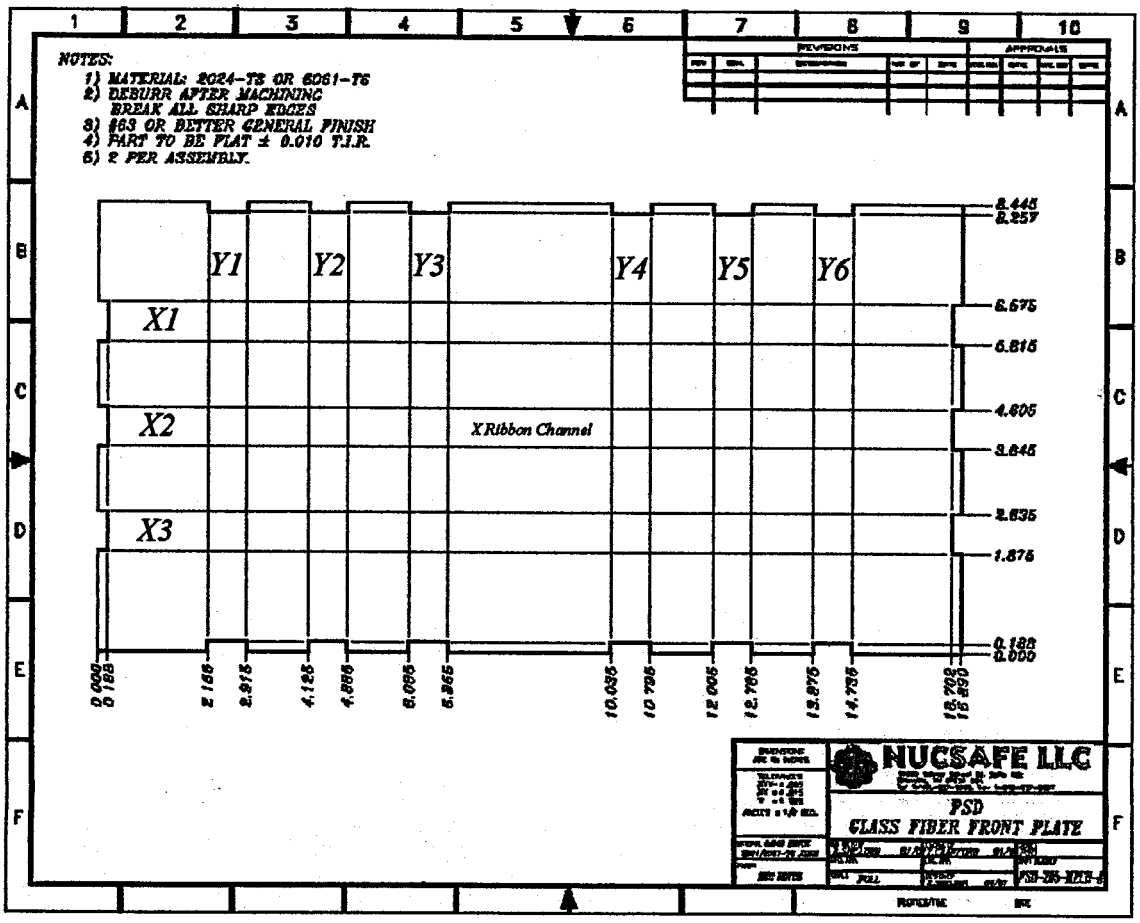

Figure 4. Mechanical drawing of the prototype position sensitive detector baseplate showing the 3 X and the 6 Y fiber ribbons channels.

The "left-hand" side of the detector baseplate, *i.e.*, the left most three Y channels and the X fiber ribbon channels shown in **Figures 2, 3,** and **4,** was designed for containing neutron sensitive scintillating glass fibers on both the X and Y ribbons. This "left detector" was produced and tested during Phase I research. During Phase II the detector baseplate will contain two types of fibers on the right hand side of the detector; neutron sensitive glass fibers on the X axis and wave shifting fibers along the Y axis. This is shown diagrammatically in **Figure 2**. This Phase I detector will then have another life for testing both the neutron glass crossed fiber sub-detector and the neutron glass – wave shifting fibers sub-detectors for 2D position sensitivity.

Subsequent to finalizing the prototype FD design, detector fabrication was undertaken at NucSafe production facilities in Oak Ridge, Tennessee. Design and machining of the baseplate and housing components of the custom detector, PMT thimbles and coupling, all electronics design and board manufacture, and system integration were performed at NucSafe. The neutron glass fiber is currently being produced using the prototype "hot drawdown" fiber drawing assembly at PNNL; this was the only process in this research that is not wholly controlled by NucSafe. The glass fiber production will be completely internalized at NucSafe facilities within the next year to 18 months (this research accelerates the implementation of this Fiber Drawing facility).

. As the detector baseplate was loaded with fiber ribbons as shown in **Figure 5**, the X & Y neutron glass fiber bilayers were interleaved; *e.g.* the first fiber bilayer ribbon was lain along the X axis (43.0 cm of active length, plus the "bare" fiber required at each end for coupling to the PMTs), then a 21.5 cm fiber bilayer ribbon on the Y axis, then another 43 cm long X Ribbon, *etc.*, until there were to be four interleaved bilayer ribbons for each X and Y detector "element."

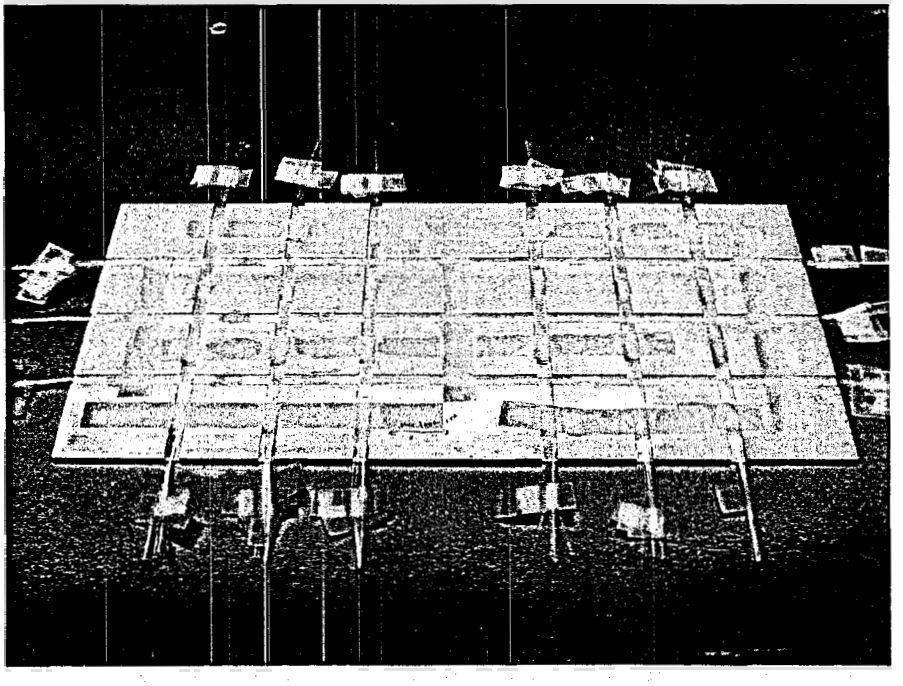

Figure 5. Prototype NucSafe position sensitive detector baseplate showing the X fiber ribbons channels and Y fiber ribbon channels being loaded with neutron glass fibers.

The detector baseplate loaded with neutron glass fibers is shown in **Figure 6.** At this point, fiber ribbons are in place and extend through the custom designed thimbles for setting the fibers in place with optical epoxide. The structural support frames were then bolted into position over the threaded thimbles (the black cylinders from which fibers protrude). **Figure 7** shows the completed detector baseplate loaded with fibers and ready for cutting off thimble ends and mounting PMTs ferrules onto the glass bound thimbles with optical coupling grease.

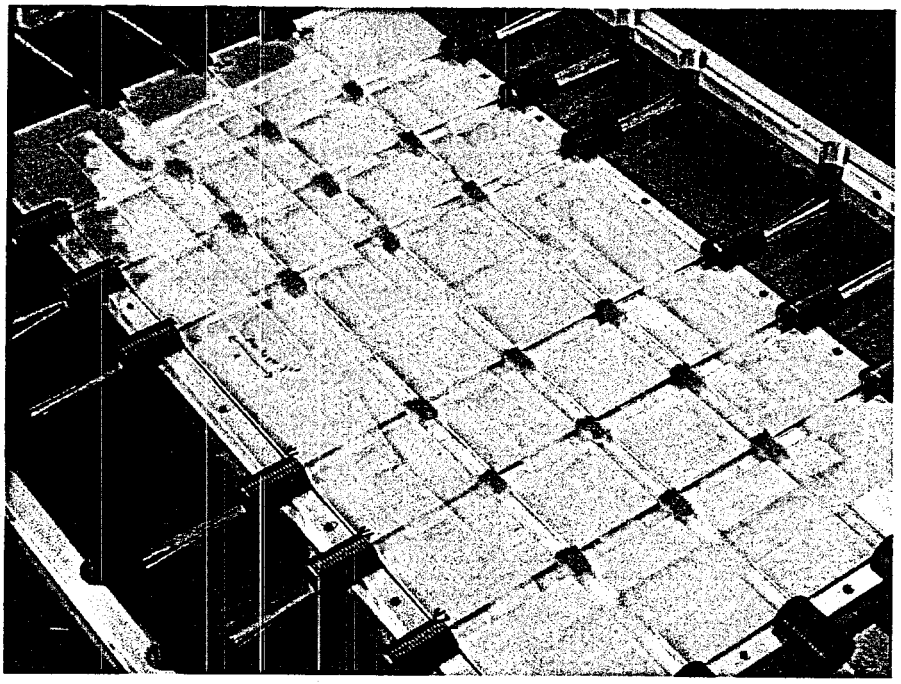

Figure 6. Detector baseplate showing filled ribbon channels with fibers protruding from PMT thimbles. The fibers were set in the thimbles with optical epoxide and the frame completed.

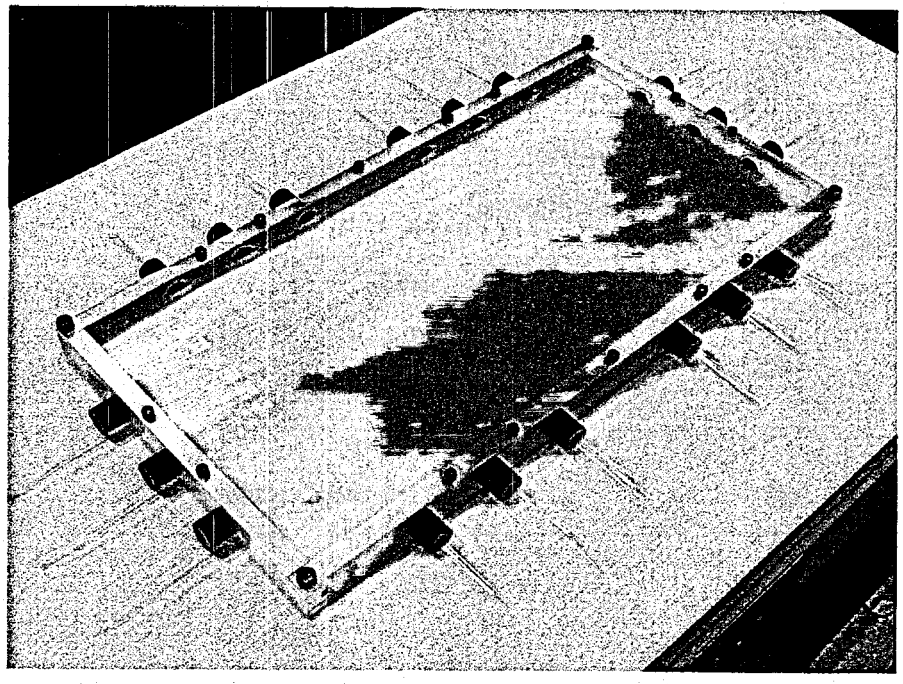

Figure 7. Assembled detector baseplate and backing. Neutron fiber ribbons extend through epoxide-set thimbles, prior to cutting thimble ends and mounting PMT ferrules.

Each individually clad neutron scintillating glass fiber is 150 μm in diameter so each 0.50 cm wide bilayer ribbon should contain ~ 65 fibers. Unfortunately, during the glass drawing process, the drum that takes up fiber in a selected overlap and spacing configuration for the fiber drawing operation was not operating properly. The amount of glass fiber that was drawn was only about one sixth of that designed for and agreed to be produced for the prototype detector ribbons. The take-up drum apparatus could not be repaired before the detector was scheduled for testing at IPNS at Argonne National Laboratory. Instead of each X and Y ribbon channel that was designed for 4 bilayers of fibers, which is approximately 260 fibers *per* X or Y ribbon, only 38 to 43 fibers were delivered *per* individual ribbon. This was considered to be a major setback as only about one-sixth the ^{6}Li atoms, would be present overall and in each ribbon. PNNL personnel could not produce more fiber given the time needed to repair the glass take-up drum, so the prototype FD was loaded with the available fiber. In spite of this major difficulty, extremely useful counting data were obtained with these few fibers. This demonstrates that the prototype detector can easily be scaled up to the full compliment of fibers for 2D testing in Phase II on both "halves" of the current detector baseplate.

The prototype position sensitive FD was completed at NucSafe production facilities. The thimbles containing the "potted" fibers were cut off perpendicular to their lengths with a diamond saw. A photomultiplier housing was designed for the specialized PMT used for this project, a Hamamatsu Series 7400 PMT that is capable of measuring individual photon events. The photomultiplier tubes were fit into ferrule housings and mounted on the threaded thimbles using optical coupling grease. The miniaturized high voltage and signal boards for each PMT were then mounted and wiring the individual PMT to connectors in the light tight detector container were completed. Mounting the detector baseplate into the light tight enclosure was the final procedure for the assembly of the prototype position sensitive fiber detector. The mounting and cabling of the PMT and the final assembly of the detector at NucSafe is shown in **Figure 8**. The exact positions of all X and Y glass fiber ribbon "detector elements" were then scribed on the front and back faces of the detector enclosure.

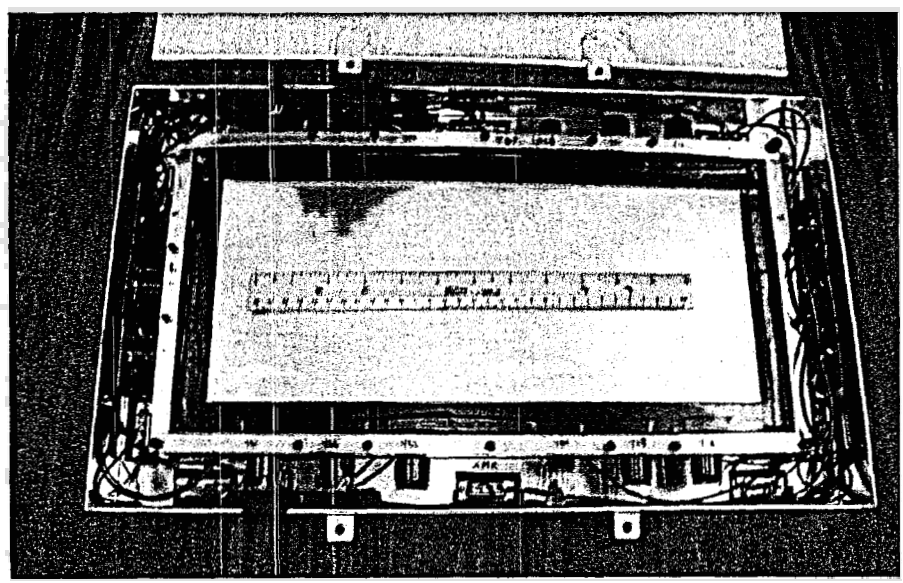

Figure 8. Newly designed miniaturized Photomultiplier Tube HV and signal boards, PMT, ferrules mounted on fiber thimbles, detector baseplate and backing in final assembly.

- Electronics Design for the Prototype Position Sensitive Fiber Detector

  - NucSafe engineers have custom designed electronics for the neutron fiber detector. Prototypes have all been developed at NucSafe with careful documentation of board designs and operational prototypes.

  - Systems boards have been designed and produced specifically for neutron glass fiber detectors. These and ancillary PC104 processing boards, high voltage power supplies, *etc.* have been integrated and thoroughly tested in the field and laboratory for over 3 years. NucSafe electronics run glass fiber systems from relatively small briefcase mounted detectors to large 5,000 to 10,000 cm^2 neutron glass panels at border stations and airports.

  - Existing board designs were extensively modified for the position sensitive detector. Two new systems boards were fabricated that are capable of simultaneous operation of 3X and 3Y ribbons; *i.e.,* for both the Phase I and Phase II prototype detectors, without additional design or modification.

  - Coincidence circuitry is applied to outputs from PMT at each end of a fiber ribbon. Coincidence criteria as well as pulse height discrimination are utilized to clearly separate the gamma and neutron signals for each ribbon that comprises a 1D detector element.

  - System boards and firmware were re-designed with additional logic chips. Logic chips were reprogrammed with the capability to compare output signals on twelve channels (3X x 3Y ribbons) in coincidence. Time slices of 160 nanoseconds are now operational for signal coincidence timing for all X and Y glass fiber ribbons in the prototype.

  - Miniaturized PMT high voltage supplies and signal amplification boards were developed and successfully tested during this project.

  - Sets of coincidence parameters can be easily uploaded to firmware. Parameters for dead time, read out rate, coincidence parameters (N_T and N_s for each PMT coincidence pair), and other settings can be quickly by the user.

  - Electronics were updated to enable data readout at three orders of magnitude faster rates. Data read out intervals for the prototype Phase I PSD could be set to 2 milliseconds (ms). The electronics designed in anticipation of Phase II research can be read out at 1 microsecond (μs) intervals; even shorter read out timing is possible.

  - A circuit for "stopping the clocks" and allowing re-acquisition of data after a user defined "lag time" has been designed and is nearing completion. System boards and timing circuits have been modified so neutron – gamma events from the "prompt pulse" at accelerator based pulsed neutron sources are not recorded. This timing delay and reacquire signal allows timing circuits of the PSD to synchronize with the prompt pulse, re-set, begin data acquisition after a given lag time (*e.g.*, 250 μm at IPNS), and keep track of "live-time." This circuit will be integrated with the system boards and operational for the first tests of the Phase II prototype.

PHASE I RESEARCH RESULTS

The Phase I prototype position sensitive fiber detector now has been tested in the laboratory at NucSafe production facilities and the Intense Pulsed Neutron Source (IPNS) at Argonne National Laboratory. Test results are summarized in this section. More detailed datasheets and the results of individual test runs produced with a variety of detector dead times, coincidence parameters, read out rates, and other user-defined parameters are available on CD from NucSafe. These data may be of interest to Technical Reviewers.

Results and Discussion of Laboratory Testing

The initial testing of the fiber detector (FD) prototype was undertaken at NucSafe production and laboratory facilities. The prototype detector system (comprised of the prototype fiber detector in a light tight enclosure, onboard electronics, cabling, system electronics, firmware, testing software, and laptop PC) operated as designed without any difficulties when first energized. The system was ready for immediate testing for response, neutron-gamma discrimination, optimizing electronic configurations, dynamic range, data read out and recording.

Two series of measurements were produced using sealed gamma and neutron sources.

1. The first measurements were run to determine whether PMTs could be adversely affected by elevated gamma and neutron fluences. Gamma interactions with PMT were of most concern with respect to detector "onboard" electronics exposed to the scattered beam.

   Gamma (^{137}Cs) and neutron-gamma (^{252}Cf) sources were placed on and near the PMT to evaluate the effects of radiation interactions with PMT and associated electronics that would be exposed to the neutron-gamma fluence of a scattered beam. Both the ^{252}Cf source, which is relatively active, and up to 50 μCi of ^{137}Cs were placed on and at varying distances from the PMT and high voltage/signal boards. PMT interactions with radiation from these sources were checked by disconnecting fiber ribbons from the PMT, masking over the ferrule to eliminate light pulses from the fiber thimbles, re-sealing the light tight enclosure and then testing the "detector-less" PMT for radiation induced interactions, subsequent to running backgrounds with the same configuration.

   The differences in the count rates with and without the sources present were statistically insignificant. No interactions in excess of those attributable from "dark noise," as given in the specification sheets for the individual PMT, were noted; even when sources were directly adjacent to PMT. Dark noise had to be considered, since the PMT was not running in coincidence mode during these tests. Neutron count rates did not increase, so elevated gamma ray fluences do not appear to adversely affect these PMT. This was encouraging as gamma fluences, even from a much "brighter" pulsed neutron source than IPNS, will not approach those emitted from the sealed sources used for lab bench testing. The conclusion drawn from these tests was that gamma rays interacting with and causing spurious counts or saturating the optoelectronic devices and associated electronics will be not be significant in a pulsed neutron source environment. Gamma interactions with FD electronics, detector, or housing components also will be tested at HFIR during Phase II research.

The PMT were re-connected to each end of the fiber ribbons and operated in coincidence mode. In all FD prototype research, pulse height discrimination 1PE was set at 100 mV and the 2PE set at an "open upper window" level for neutron gamma interactions with the fiber. These settings have been determined to be optimal and confirmed during years of fiber detector operations and testing, so were not altered during tests of the FD.

2. The second series of laboratory tests were to evaluate the prototype response and ability to discriminate gamma interactions from neutron captures. Numerous gamma and gamma/neutron measurements were collected for each set of dead time (DT) and coincidence parameters N_T and N_S. Both ^{137}Cs and ^{252}Cf sources were used.

   Each of the 5 ribbons (3 X and 2 Y in the Phase I prototype) were tested for increased count rates and "spilling over" of counts into the neutron channel when ribbons and ribbon intersection "nodes" were exposed to ~50 μCi of ^{137}Cs at distances as short as 8 mm. Gamma counts increased since the neutron glass is slightly gamma sensitive, but pulse height discrimination and coincidence circuits rejected gammas from spilling over into the neutron channel. Some settings rejected virtually all gammas from the neutron channel. Each set of dead time (DT) and coincidence parameters (N_T and N_s) parameters was measured for relative neutron-gamma totals and ratios. Two data read out rates were also tested. Similar measurements were then performed for each of 3 X and 2Y interfaced ribbons and all ribbon intersection "nodes" using ^{137}Cs sources and ^{137}Cs plus moderated ^{252}Cf sources.

   Table 1 is a listing of coincidence parameter sets and comments for data sets acquired using the moderated ^{252}Cf source. *The detection and integration times are combined, so the DT listed is actually the total signal processing time for an interaction.* The minimum DT for Phase I electronics was 640 ns; Phase II electronics could be on the order of 160 ns, but faster measurements are limited by the Ce^{3+} fluorescence relaxation time. N_{Total} (N_T) and N_{Side} (N_S) refer to the number of total photons (N_T) and the number of photons detected at PMTs at each "side" of the fiber ribbon (N_S) within the set time domain that are required to "count" an interaction as a neutron capture. The results of these tests, given in **Table 1**, were used to identify discrimination settings of most interest for testing at IPNS.

TABLE 1
Dead time and Discrimination Settings Tested for the Fiber Detector Prototype

Electronic Conf.	Dead Time (DT) in ns, $N_{Total\ (NT)}$, $N_{Side\ (NS)}$	Read Out Rate (ms)	n/γ Ratio on X (Normalized)	Comments
0	1600, 4, 1	2	1.74	□ to Conf. 7, γ lower
1	1600, 4, 1	5	1.64	Read out too long
5	1600, 4, 0	2	2.56	n counts higher, γ lower
7	640, 4, 1	2	1.43	n □ Conf. 0, γ higher
8	640, 4, 1	5	1.42	Read out too long
9	640, 3, 0	2	2.73	n < Conf. 5

Results of n – γ discrimination parameter settings shown in **Table 1** make sense. Lower count rates were expected for Configuration 5 and 8 in a pulsed source because of the slow read out rate, rather than due to coincidence settings. Read out rates longer than 1 or 2 ms are not useful for testing at IPNS where the prompt pulse of 250 μs is followed by 30 ms of utilizable data. The 5 ms read out interval will "cut off" data and cause "smearing" of the prompt data into another 5 ms read out interval unless the clocks for the detector system and pulsed source are synchronized. Regardless, data would not be collected during the 5 ms interval that contains prompt data (~17% of the measurement time), so count data and effective live time decrease. This illustrates the necessity to read out data for pulsed sources in short intervals; 250 μs being the shortest time interval required at IPNS, assuming the detector and prompt signal timing are synchronized; a lot of data if long counts are involved. A compromise of 1 ms for data read outs will likely suffice, but advice on this point will be sought from SNS and IPNS research scientists.

The electronic Configurations 0, 7, and 9 show the best responses for discrimination, with 0 and 7 likely to be the best settings for testing in a pulsed source environment. This is also makes sense since the Nt=4, Ns=0 settings and Nt=3 and Ns=0 (Conf. 5 and 9, respectively) have higher neutron count rates and lower gamma count rates as expected for these less stringent coincidence requirements - some gammas are being counted as neutrons. The difference in "spill over" for the least stringent (Conf. 5 and 9) *versus* the most stringent coincidence settings (Conf. 0 and 7) is about 12%. Overall, Conf. 7 has the best n – γ discrimination statistics based on the data obtained while using the ^{252}Cf source. Coincidence settings for Configurations 7 and 9 were focused upon for testing at IPNS to discern maximum and more conservative count rates. The longer 1600 ns DT version of Conf 7 is Conf. 0, which has about identical neutron count rates and slightly lower gamma counts. All these configurations demonstrate that a longer DT setting decreases the gamma count rate with less impact on the neutron rate; whereas lower N_T and N_S, especially N_S=0, contribute to a few gammas being counted as neutrons.

These sets of measurements also demonstrated the position sensitivity of the ribbons in 1D and 2D. Measurements of the ^{252}Cf on specific X and Y ribbons and ribbon nodes were recorded for various configurations primarily for the purpose of setting coincidence parameters as discussed. Another observation was that the X and Y ribbons had significantly higher counts rates when the moderated source was placed directly over the ribbon. This was, of course, expected for individual ribbons. When the source was placed on a node, both the X and Y ribbons intersecting at the node had count rates that were almost as high as when the source was over a single ribbon. When the moderated source was collimated as well as possible over a node, the signals on the other X and Y ribbons not intersecting at the node decreased to near background levels for the measurements. None of these results for node measurements were particularly surprising and were expected; however, it was reassuring to directly observe the 1D sensitivity for individual arrivals for both X and Y ribbons and corresponding arrivals in the same time increment on the orthogonal ribbon.

The laboratory testing was quite useful in demonstrating the neutron fiber detector responded well at count rates produced by an active gamma-neutron source. Neutron – gamma discrimination for the prototype FD is very effective in high gamma fluences, at least for the number of fibers now comprising individual ribbons. Counting results using a variety of electronic configurations were completed and the most favorable configurations defined for testing at the Pulsed Neutron Source.

Results and Discussion of Testing at IPNS

The next phase of testing was at the Intense Pulsed Neutron Source at Argonne National Laboratory. The PI contacted Dr. R Kent Crawford who suggested that NucSafe work with Dr. Ron Cooper at IPNS. The entire IPNS staff and especially Dr. Cooper have been very helpful in the experimental portion of this study and have dedicated a significant amount of time to assure that the detector could be tested at IPNS in a timely manner. Beam line testing of the prototype had initially been discussed with Dr. Mohana Yethiraj of JINS and was planned to be conducted at HFIR. Dr. Yethiraj kindly offered to assist in the development of experiments for testing the FD at HFIR in Oak Ridge. However, the beryllium reflector change at HFIR has taken longer than expected. Testing at HFIR as well as at IPNS has been included in the Phase II research plan.

The PI tested the prototype FD in the HPID/QUIP gate during March 2001. Ron Cooper assisted the PI set up for measurements in beam line areas and provided many useful suggestions. A rod of polyethylene in the QUIP beam line was used to scatter neutrons for testing the FD. The sample well dimensions were obtained prior to finalizing the detector design, so the FD fit into the QUIP sample well enclosure without any problems. The front of the detector was placed 46 cm (18 inches) from and perpendicular to the midline of the QUIP gate. The system electronics were placed above the sample well on the sidewall shielding. The top shielding that covers the sample well was not in place for any measurements – the detector had to be accessed on numerous occasions for masking the front of the detector. **Figure 9** shows the FD in place for full detector measurements in the IPNS QUIP gate.

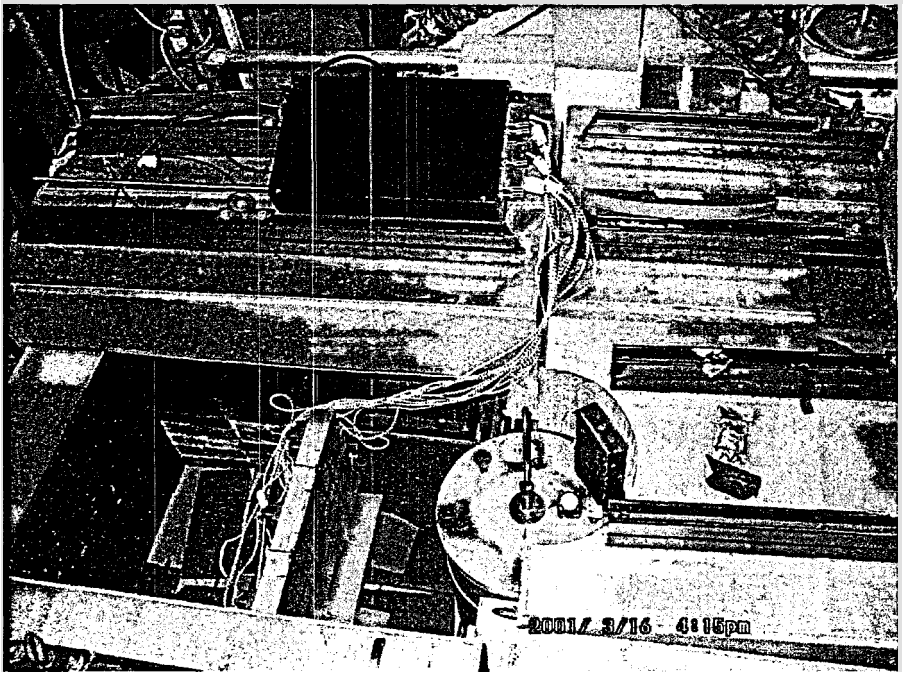

Figure 9. Fiber Detector in the QUIP sample well at IPNS. Exact locations of X and Y fiber ribbons are marked on the detector enclosure. The system electronics black box is above the well sidewall shielding (photo by Ron Cooper).

System electronics used for the Phase I tests enabled coincidence measurements on all 3 X ribbons and both Y ribbons, but not on all X-Y ribbons in "2D coincidence." The number of operational Y ribbons decreased from 3 to 2 for these tests in order to begin enabling the X – Y coincidence logic circuits and re-programming the logic chips to compare 12 inputs for each time interval. This is one type of X-Y coincidence that will be tested for determining 2D interactions for individual neutron captures within 640 ns or less (160 ns is the goal in Phase II). The signal timing circuit was being completed so the detector could "time-out" for 250 μs during the pulse at IPNS. Pulse data was effectively filtered from the IPNS measurements.

At least 30 measurements were taken in each configuration of interest, each measurement consisting of a total of 3600 individual data records for each of the X and Y fiber ribbons. Data were recorded in either 2 ms or 5 ms intervals as *per* the configuration being tested. The same numbers of background measurements were recorded with the beam line gate closed for each electronic configuration and represent the instrumental background in the sample well for each configuration. A standard deviation of the mean has been calculated for individual ribbons in each set of measurements. In excess of 50,000 individual 2 ms measurements were recorded for both the X and Y fiber ribbons in each configuration. The total of the 30 measurements represents about 100 seconds of live time for that configuration. Instrumental background measurements have been subtracted and uncertainties due to standard deviations of the means and have been propagated along with the uncertainties from background counts. Instrumental backgrounds have been subtracted from the gross counts of the "Gate Open Full Detector" and uncertainties have been propagated accordingly where indicated in data tables. Data presented in Tables in this section are predominately compilations of data reports drawn from the MS Access™ databases used to handle and sort the data. Copies of raw data for all the IPNS measurements (hundreds of files containing nearly one million data records), parsed data in MS Excel™ Worksheets (hundreds of sheets), and the Access database (~96 Mb) have been archived and can be provided to reviewers on CD if requested.

The first sets of measurements were of the "Full Detector," *i.e.*, measurements for all glass ribbons without any "masking." These measurements were of great interest since the inadvertently sparse fibers in glass ribbons significantly decreased the sensitivity of the prototype detector. The fibers captured scattered neutrons much more effectively than expected considering each ribbon is made up of only 38 to 43 fibers *vice* the ~260 as planned and designed for. These full detector measurements were performed for all tested electronic configurations and test data are presented in **Table 2. Table 2** (shown on the following page) is a compilation of neutron and gamma count rates given in counts *per* second (cps) for all coincidence settings and data read out rates tested at IPNS. The first point of interest is the relatively high count rates in both the X and Y sets of glass ribbons considering the number of fibers. This is very encouraging, as the detector baseplate can easily be scaled up with additional fibers in the early Phase II R&D. Other notable points are the consistently lower count rates for the X2 ribbon and also, to a lesser degree, the Y1 ribbon compared to that of the Y3 ribbons. This is likely due to differing numbers of fibers in ribbons – the least in X2 and somewhat less in Y3; with this few fibers, a deficient of just 4 to 5 could make ~10 - 15% difference in thermal neutron captures. The count rates for the X and Y ribbons must be considered separately, as the Y ribbons are only half the length as X ribbons and should have about half the count rates (half the ^{6}Li atoms) for full detector measurements, ignoring parallax issues. However, Y ribbons neutron count rates are just 12 – 18% less than for X ribbons.

TABLE 2

Neutron and Gamma Measurements of Scattered Neutrons from the QUIP Beam made with the Phase I Prototype Fiber Detector for "Gate Open Full Detector"
Gamma (G) and Neutron (N) Count Data are Given in Counts *per* Second (cps)
Data are Background Corrected Except were Noted

Configuration	X1 and Y1 Ribbons		X2 Ribbon		X3 and Y3 Ribbons	
7	G1	N1	G2	N2	G3	N3
X	30.7	47.2	32.4	40.5	31.8	47.7
+/- (1σ)	0.6	0.7	0.6	0.6	0.6	0.7
Y	23.3	36.3	DT = 640 ns, 2 ms		27.8	42.6
+/-	0.5	0.7	N_{Total} = 4, N_{Side} = 1		0.5	0.7
0	G1	N1	G2	N2	G3	N3
X	25.9	49.9	28.2	41.9	27.2	49.3
+/-	0.5	0.7	0.5	0.7	0.5	0.7
Y	19.1	38.8	DT = 1600 ns, 2 ms		21.3	43.7
+/-	0.4	0.6	N_{Total} = 4, N_{Side} = 1		0.5	0.7
9	G1	N1	G2	N2	G3	N3
X	18.2	50.7	16.9	47.2	19.5	51.0
+/-	0.5	0.7	0.4	0.7	0.5	0.7
Y	14.6	38.9	DT = 640 ns, 2 ms		19.1	42.4
+/-	0.4	0.6	N_{Total} = 3, N_{Side} = 0		0.5	0.7
5	G1	N1	G2	N2	G3	N3
X	20.1	55.0	21.6	48.2	19.4	53.6
+/-	0.5	0.7	0.5	0.7	0.5	0.7
Y	14.4	40.8	DT = 1600 ns, 2 ms		17.1	45.3
+/-	0.4	0.6	N_{Total} = 4, N_{Side} = 0		0.4	0.7
8 Not Corr	G1	N1	G2	N2	G3	N3
X	22.3	34.2	22.7	29.0	23.2	33.4
+/-	0.5	0.6	0.5	0.5	0.5	0.6
Y	15.9	23.7	DT = 640 ns, 5 ms		18.0	27.7
+/-	0.4	0.5	N_{Total} = 4, N_{Side} = 1		0.4	0.6
1 Not Corr	G1	N1	G2	N2	G3	N3
X	18.5	33.3	20.8	28.1	18.3	33.2
+/-	0.5	0.6	0.5	0.6	0.5	0.6
Y	13.0	25.0	DT = 1600 ns, 5 ms		14.4	28.2
+/-	0.4	0.5	N_{Total} = 4, N_{Side} = 1		0.4	0.6

The higher than expected count rates in Y ribbons is believed to be due to more photons in the shorter fibers reaching the PMT. The intensity of light reaching fiber ends as a function of fiber length is well defined for this glass so this hypothesis can be tested. This points out the advantage of using X and Y fibers of equal lengths to produce square planar or concave detector elements. X and Y fiber ribbons with different lengths may require different coincidence settings as well; another reason for square detector array elements. Another point of interest in IPNS data is that the coincidence settings noted as most favorable in lab tests with sealed sources seems to hold up for scattered neutrons. Configurations 7 and 0 seem to be the most conservative for neutron – gamma discrimination followed by Configuration 9 with slightly higher counts discriminated as neutron and lower gamma ray counts. Configurations 1 and 8 are not useful for the reasons suspected during laboratory evaluation; data is lost in the long read out times tied to the prompt pulse. A last general point is evident as well. The gamma count rates are believed to be somewhat elevated because the prompt pulse is fairly well, but not completed filtered from the data. This will be evaluated in Phase II when the gating signal circuit is fully integrated with timing circuits on the system boards.

The other tests conducted at the QUIP gate involved masking off the detector face and making measurements of specific detector ribbons and nodes to demonstrate position sensitivity. It was uncertain if count rates would be sufficient for these tests given the few fibers *per* ribbon, until the first full detector measurements had been made and data reduced. Measurements of an isolated Y axis strip and ribbon intersection nodes were then undertaken. The results of measurements made with the detector face fully masked with 5 cm thick borated paraffin (BP) bricks are shown in **Table 3**.

TABLE 3

Neutron and Gamma Measurements of Scattered Neutron from the QUIP Beam made with the Masked Phase I Prototype Fiber Detector for "Gate Open Full BP Mask"
Gamma (G) and Neutron (N) Count Data are Given in Counts *per* Second (cps)

Configuration	X1 and Y1 Ribbons		X2 Ribbon		X3 and Y3 Ribbons	
7 0711 HRS	G1	N1	G2	N2	G3	N3
X	7.8	6.5	7.1	6.3	8.6	8.1
+/- (1σ)	0.3	0.3	0.3	0.2	0.3	0.3
Y	6.5	7.0			6.7	7.0
+/-	0.2	0.3			0.3	0.3
7 1058 HRS	G1	N1	G2	N2	G3	N3
X	7.1	6.3	6.3	5.5	7.0	6.6
+/-	0.3	0.3	0.3	0.2	0.3	0.3
Y	6.6	6.5			7.1	6.3
+/-	0.3	0.3			0.3	0.3
9	G1	N1	G2	N2	G3	N3
X	6.8	9.3	6.1	8.5	7.2	9.3
+/-	0.3	0.3	0.2	0.3	0.3	0.3
Y	4.1	8.5			5.5	7.7
+/-	0.2	0.3			0.2	0.3

Measurements with just the Y1 fiber ribbon exposed (see note below) in two electronic configurations and the results of subtracting measurements of the fully masked detector are given in **Table 4**. It is granted that uncertainty is introduced by taking measurements in which X or Y ribbons or nodes are "exposed" while the remainder of the detector remains masked and then subtracting the measurements taken with a full detector mask to arrive at a result representative of

TABLE 4

Neutron and Gamma Measurements of Scattered Neutrons from the QUIP Beam Made with the Partially Masked Phase I Prototype Fiber Detector for "Gate Open Y1 Exposed"

Gamma (G) and Neutron (N) Count Data are Given in Counts *per* Second (cps)

Configuration	X1 and Y1 Ribbons		X2 Ribbon		X3 and Y3 Ribbons	
Y1 Ribbon Exposed. Remainder of Detector Face Masked with Borated Paraffin Bricks						
7	G1	N1	G2	N2	G3	N3
X	8.2	9.0	7.3	8.5	8.6	9.3
+/- (1σ)	0.3	0.3	0.3	0.4	0.3	0.4
Y	14.9	29.8			7.7	6.9
+/-	0.4	0.5			0.2	0.2
Y1 Ribbon Exposed Minus Detector Face Fully Masked with Borated Paraffin Bricks- 0711						
7 0711 HRS	G1	N1	G2	N2	G3	N3
X	0.5	2.5	0.2	2.2	-0.1	1.2
+/-	0.4	0.4	0.4	0.5	0.4	0.5
Y	8.4	22.8			1.0	-0.2
+/-	0.4	0.6			0.3	0.4
Y1 Ribbon Exposed Minus Detector Face Fully Masked with Borated Paraffin Bricks - 1058						
7 1058 HRS	G1	N1	G2	N2	G3	N3
X	1.1	2.8	1.0	3.0	1.5	2.7
+/-	0.4	0.4	0.4	0.4	0.4	0.5
Y	8.3	23.2			0.6	0.6
+/-	0.4	0.6			0.4	0.4
Y1 Ribbon Exposed. Remainder of Detector Face Masked with Borated Paraffin Bricks						
9	G1	N1	G2	N2	G3	N3
X	5.2	11.2	4.5	10.4	5.9	11.3
+/-	0.2	0.3	0.2	0.3	0.2	0.3
Y	11.8	31.4			5.6	7.0
+/-	0.3	0.5			0.2	0.3
Y1 Ribbon Exposed Minus Detector Face Fully Masked with Borated Paraffin Bricks						
9	G1	N1	G2	N2	G3	N3
X	-1.6	1.9	-1.6	1.9	-1.3	1.9
+/-	0.3	0.4	0.3	0.4	0.4	0.4
Y	7.6	22.8			0.1	-0.7
+/-	0.4	0.6			0.3	0.4

the fiber ribbon or node. However, for this proof of principal testing, beam time was limited and a computational "stripping" of the mask data can provide useful insights into the position sensitive response. Two sets of measurements were performed while the Y1 ribbon was exposed to the scattered beam and the remainder of the detector face was masked with the borated paraffin bricks. The Y1 ribbon and an additional 1 cm on each side of the ribbon position as indicated on the detector enclosure was left exposed. At least, the intent was to leave the Y1 ribbon exposed. As can be seen from photographs of the detector base and light tight enclosure, some parallax problems arise since the detector is about 7 cm thick. The distance from the front enclosure to the fiber ribbon channels in the base plate is about 1.7 cm. The shielding also presents some problems with masking Y oriented ribbons that are off the center axis of the beam gate. The borated paraffin bricks are 5 cm thick, so the Y1 ribbon may not have been fully exposed. This added another lesson learned from Phase I research; make the detector elements thin to avoid parallax problems.

Figure 10 is a graphical representation of data collected in Conf 7. with the Y1 ribbon exposed after stripping off the full mask data. These types of bar charts are useful for quickly interpreting the position sensitivity measurements, but can be misleading without understanding what is actually plotted on the nodes. The entire Y1 ribbon had about 23 neutron counts *per* second (cps). X ribbons, all of which were masked except directly adjacent to the Y1 ribbon, had only ~2 cps after the stripping of the full mask data (**Table 4**). The combination of theY1 count rate and the data for each of the X ribbons sum to the count rates plotted on the 3 X-Y1 intersection nodes. A similar summation yields the 3 X-Y3 ribbon node values. Although not ideal, the diagram gets the point across in a simplistic way for comprehending the significantly higher count rates for exposed ribbons. Similar diagrams can be produced for the remaining two sets of measurements and then subtracting data for the masked detector using the same settings.

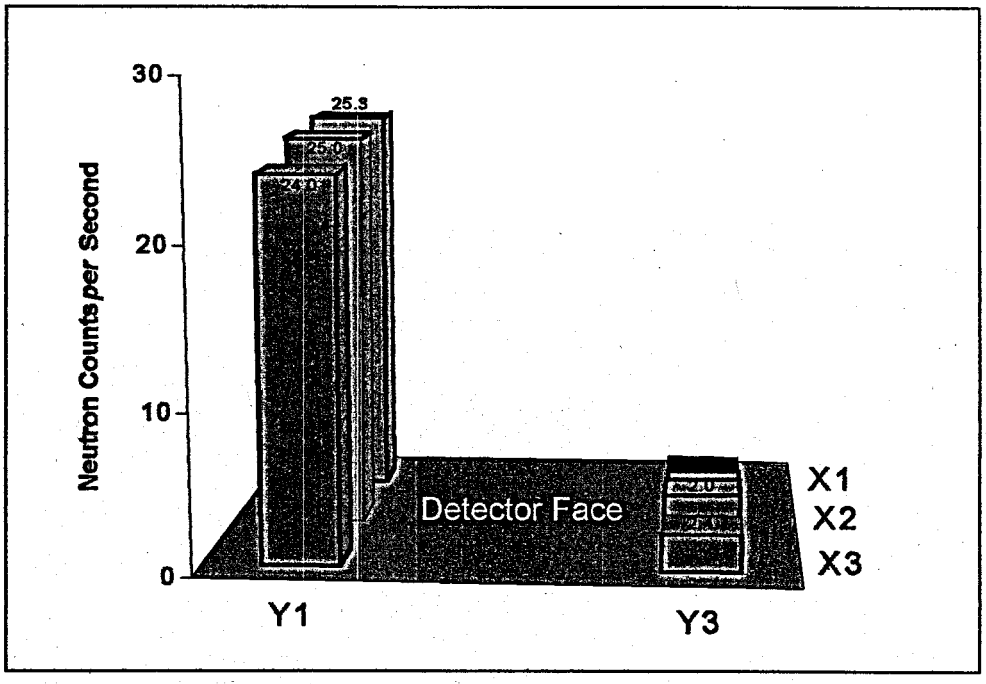

Figure 10. Graphical representation of neutron count rates into ribbons for the Y1 Exposed Ribbon measurements minus the full borated paraffin mask for Configuration 7 (0711 Hrs data – see **Table 4**).

Figure 10, depicting the "remainder" resulting from stripping off the full borated paraffin mask from the Y1 Exposed measurements, show the count rates for this ribbon are clearly elevated, having count rates in excess of twice that of all other ribbons combined. Data from two configurations are given in **Table 4** as well as two independent sets of measurements of the fully borated paraffin mask in Conf. 7. The counts rates for the Y1 ribbon exposed in both electronic configurations are quite elevated, but not as high as for the rates of the same fiber ribbon for the full detector face measurements summarized in **Table 2**. The Y1 "stripped mask" values are about 23 cps for neutrons in both Conf. 9 and 7 (both masks), but are about 39 and 36 cps for the Y1 ribbon for Conf. 9 and 7, respectively, in full detector measurements. This is believed to be due to unintentional partial masking of Y1 as discussed above.

Data was also collected for specific glass ribbon intersection nodes on the detector while the remainder of the detector face remained masked with borated paraffin bricks. The same rationale was applied to computationally strip away the fully masked detector measurements. Two nodes were observed; one was measured with two electronic configurations. The X1-Y1 node (*i.e.*, the intersection of the X1 and Y1 fiber ribbons, see **Figures 2** and **4**) and the X2-Y3 node were measured while exposed and the remainder of the detector was masked. Count rate data for these measurements are given in **Table 5**.

TABLE 5

Neutron and Gamma Measurements of Scattered Neutrons from the QUIP Beam Made with the Phase I Prototype Fiber Detector for X2-Y3 and X1-Y1 Node Data

Gamma (G) and Neutron (N) Count Data are Given in Counts *per* Second (cps)

Configuration	X1 and Y1 Ribbons		X2 Ribbon		X3 and Y3 Ribbons	
X2-Y3 Node Exposed, Conf. 7						
7	G1	N1	G2	N2	G3	N3
X	6.0	7.0	8.2	16.0	7.9	8.3
+/- (1σ)	0.3	0.3	0.3	0.4	0.3	0.3
Y	6.7	6.1			7.3	10.8
+/-	0.3	0.3			0.3	0.3
X2-Y3 Node Minus Full BP Mask Conf 7, 0711 HRS						
7	G1	N1	G2	N2	G3	N3
X	-1.7	0.5	1.1	9.7	-0.7	0.2
+/-	0.4	0.4	0.4	0.5	0.4	0.4
Y	0.2	-0.8			0.6	3.8
+/-	0.4	0.4			0.4	0.4
X2-Y3 Node Minus Full BP Mask Conf 7, 1058 HRS						
7	G1	N1	G2	N2	G3	N3
X	-1.1	0.8	2.0	10.6	0.9	1.7
+/-	0.4	0.4	0.4	0.5	0.4	0.4
Y	0.1	-0.4			0.2	4.5
+/-	0.4	0.4			0.4	0.4

TABLE 5 (Cont'd.)
Neutron and Gamma Measurements of Scattered Neutron from the QUIP Beam made with the Phase I Prototype Fiber Detector for X2-Y3 and X1-Y1 Node Data (cps)

X2-Y3 Node Exposed, Conf. 9						
9	**G1**	**N1**	**G2**	**N2**	**G3**	**N3**
X	4.3	9.3	5.8	19.0	5.9	10.1
+/-	0.2	0.3	0.3	0.5	0.3	0.3
Y	4.3	7.5			7.5	13.2
+/-	0.2	0.3			0.3	0.4
X2-Y3 Node Minus Full BP Mask, Conf. 9						
9	**G1**	**N1**	**G2**	**N2**	**G3**	**N3**
X	-2.5	0.0	-0.3	10.5	-1.3	0.8
+/-	0.3	0.4	0.4	0.5	0.4	0.5
Y	0.2	1.0			0.4	7.7
+/-	0.3	0.4			0.4	0.5
X1-Y1 Node Exposed, Conf. 9						
9	**G1**	**N1**	**G2**	**N2**	**G3**	**N3**
X	9.1	16.8	4.8	8.8	6.3	9.2
+/-	0.3	0.4	0.2	0.3	0.3	0.3
Y	5.9	13.8			5.8	7.9
+/-	0.3	0.4			0.3	0.3
X1-Y1 Node Minus Full BP Mask, Conf. 9						
9	**G1**	**N1**	**G2**	**N2**	**G3**	**N3**
X	2.3	7.5	-1.3	0.4	-0.9	-0.2
+/-	0.4	0.5	0.3	0.4	0.4	0.4
Y	1.7	5.3			0.2	0.2
+/-	0.4	0.5			0.4	0.4

The nodal data are interesting as well. Keeping in mind the uncertainties introduced by stripping off the masked detector data, a few observations can still be made. The count data in **Table 5** for individual nodes are statistically significant, even with one-sixth of the fibers than planned. Count rate data from the X2-Y3 node and the X1-Y1 node clearly show position sensitivity on the exposed nodes, as expected for the fully populated ribbon channel, but considered to be unlikely for the prototype detectors with one-sixth the fiber. However, the count rates were better than expected, perhaps too good, considering the lengths of fiber ribbons exposed and the difficulties in masking the full detector except for a area about 16 cm^2 around the node centroid. Getting the gap in the mask to roughly equal lengths along X and Y axes was difficult due to the size and thickness of the borated paraffin bricks.

Figures similar to that plotted for the Exposed Y1 ribbons can also be produced for these nodal data, but an additional constraint is added since the detector faces are masked everywhere except 1 node of the 6 on the 3X x 2Y fiber ribbon prototype. Whereas, the nodal data for the Exposed Y1 ribbon can be summed similar to matrix addition, degrees of freedom have been

decreased for individual X-Y nodes. For example, a 3D bar chart of the neutron counting rates for the X2-Y3 node for Conf. 7, subsequent to stripping off the full mask data for the 1058 Hrs set of measurements for the mask, yields the plot shown in **Figure 11.** It must be recalled when interpreting this Figure that nodal data that have been summed for graphical presentation were constrained to single dimensional components for 3 of the 6 nodes. In this instance of the X2-Y3 node being exposed, the nodal data plotted on the X2-Y1, X1-Y3, and X3-Y3 nodes are single dimension components, otherwise the entire X2 and Y2 ribbons will appear to be credited with the count data that was constrained to just the X2-Y3 node by masking. These types of plots are a simplistic way of plotting these data, but can lead to misinterpretations if the plotting method is not considered. This graphical artifact will not be an issue when data from individual neutron arrivals at hundreds of nodes are obtained with the higher resolution detectors planned for Phase II research and development.

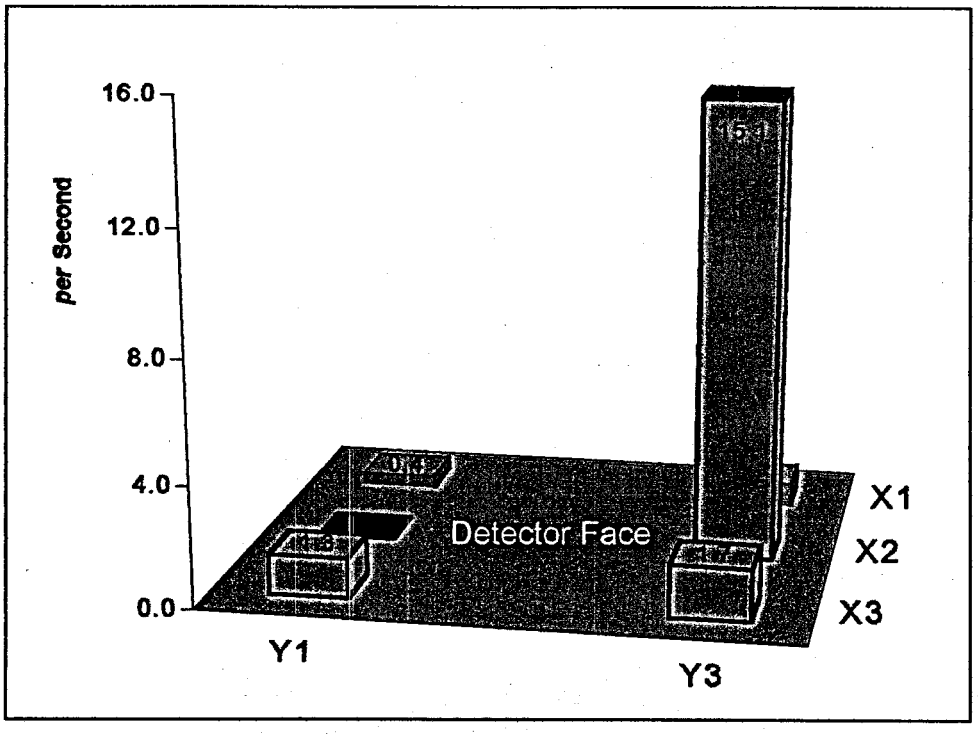

Figure 11. Graphical representation of neutron counts into exposed X2-Y3 Node minus the full mask for Configuration 7 (1058 Hrs mask data).

Neutron count rate data from the measurements of the X1-Y1 node collected with the coincidence electronic setting in Configuration 9 are shown on the following page in **Figure 12.** These data are remainders of counting with the detector face masked except 4.4 cm on the X axis and 4.2 cm on the Y axis around the X1-Y1 node and then subtracting the count rates for the full detector when completely masked with borated paraffin bricks collected using identical coincidence settings (Configuration 9). The data have been "smoothed" as before; *i.e.*, for the X1-Y1 node case, the X1-Y3, X2-Y1, and X3-Y1 data nodes contain count data only from one dimensional component.

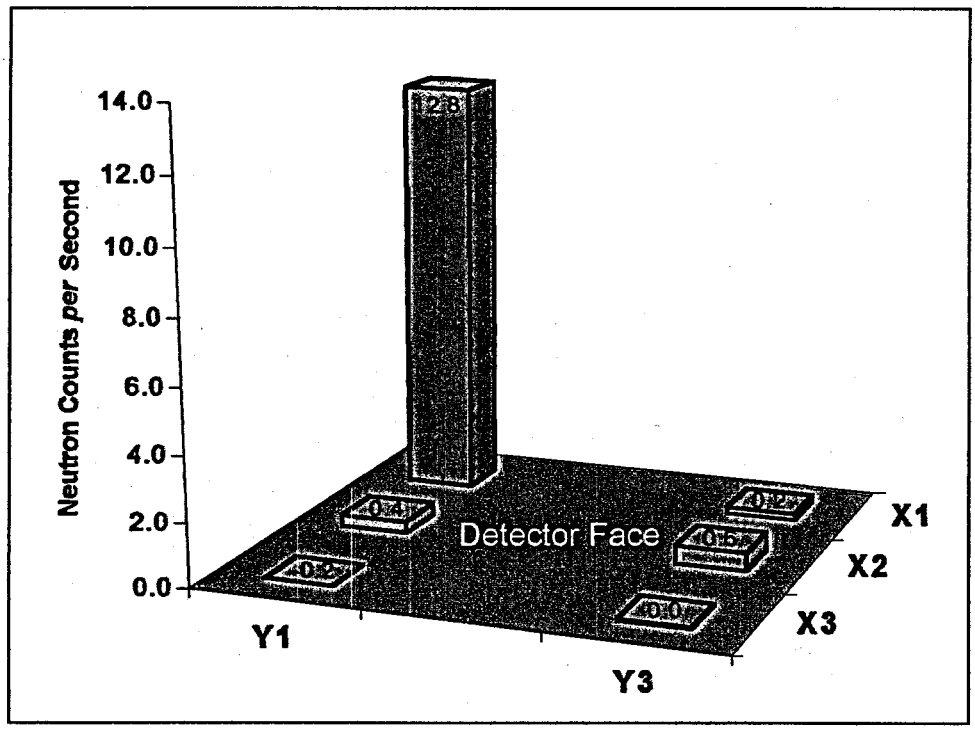

Figure 12. Graphical representation of neutron counts into exposed X1-Y1 Node minus the full mask for Configuration 9.

The comment made in an earlier paragraph with regard to the count rate data being "too good" for nodal data should be elaborated upon.

X2-Y3 Node

Neutron count rate data shown for the X2-Y3 nodal data after subtracting the Fully Masked Detector data using the same setting and 1058 Hrs mask measurements were 10.6 ± 0.5 (1σ) neutron counts *per* second (cps) at X2 and 4.5 ± 0.4 (1σ) neutron cps on Y3 (**Table 5**), summing to 15.1 neutron cps on the X2-Y3 node (see **Figure 11**). As mentioned, about 4 cm of both the X and Y ribbons were exposed about the node (~2 cm on either side of the intersection point) when the detector face was masked for nodal measurements using borated paraffin bricks. The neutron count rate for the entire X2 ribbon in this configuration (see **Table 2**) was 40.5 ± 0.6 (1σ) (recall that the X2 ribbon has the lowest neutron count rate for a "Full Detector" measurement due to fewer fibers in the ribbon). Therefore, it was expected that the X2 nodal count rate for 4.4 cm of exposed X2 ribbon about the X2 node, would be about one-tenth the total ribbon count rate since an X ribbon has an "active length" of 43.0 cm. What was indirectly observed was ~26% of the neutron count rate for the entire X2 fiber ribbon was detected when ~10% of the ribbon was exposed.

Conversely, the neutron count rate data for the entire Y3 ribbon in Conf. 7 was 42.6 ± 0.7 (1σ) cps (**Table 2**) and the count rate for the 4 cm of the fiber ribbon around the Y3 node was 4.5 ± 0.4 (**Table 5**) or ~11% of the rate for the entire ribbon when about 19% of the length was

exposed (Y ribbons have 21.5 cm of "active length"). The discrepancy in the lower count rate than expected for the Y3 node is not gross, considering that the mask data has been subtracted so uncertainties are introduced, plus parallax issues are involved as discussed earlier. So a lower than expected count rate is not too difficult to explain, but double the expected count rate on the X2 node is not. In short, the X2 node data are difficult to understand and neutron count rates on the ribbons that comprise the X2-Y3 node seem to be the opposite of what was expected intuitively.

It had been noted that the Full Mask data for Conf. 7 1058 Hrs measurements were not as complete and consistent as other mask data, so additional nodal data have been examined in more detail. The X2-Y3 nodal data collected in Conf. 7 and then stripping the Full Mask data for Conf. 7 0711 Hrs are somewhat lower for the X2 and Y3 nodal data, but remain significantly higher on X2 than expected from the length of the X2 ribbon exposed during the measurements.

X1-Y1 Node

The X1-Y1 nodal data (in Conf. 9), the "Fully Masked" and "Full Detector" data for Conf. 9 can be examined in a similar manner. The "Full Detector" neutron count rates (all in cps) for Conf. 9 on the X1 ribbon was 50.7 ± 0.7 (1σ) and 38.9 ± 0.6 on the Y1 ribbon (**Table 2**) whereas the X1 nodal data, subsequent to subtracting the "Full Mask" for Conf. 9 was 7.5 ± 0.5 (1σ) and the Y1 nodal data was 5.3 ± 0.6 (**Table 5**). As in previous nodal measurements, about 4 cm of each ribbon was exposed around the node, about 2 cm to either side of the X1 and Y1 ribbons at the X1-Y1 node. The count rate for the X1 nodal data was ~14.8 ± 1.0% of the full X1 ribbon count rate when 10.2% of the full ribbon was exposed. The Y1 nodal count rate was 13.6 ± 1.3% of the full Y1 ribbon count rate when 19.5% of the ribbon was exposed. As discussed previously, a slightly lower than expected count rate for the exposed Y1 ribbon around the node is not too troublesome and may be attributable to parallax issues and masking. The somewhat higher than expected count rate on the X1 ribbon about the node is not as appreciable as for the X2-Y3 node; however, the higher count rate still requires an explanation. More extensive testing of the Fiber Detector at IPNS in Phase II R&D should shed light on the higher than expected neutron count rates on the X fibers when nodal data are collected.

SUMMARY AND CONCLUSIONS

The Phase I prototype Fiber Detector worked quite well and better than expected given the number of neutron glass fibers *per* ribbon. The Phase I research delivered far more than anticipated. In fact, many goals that were expected to be undertaken in the Phase II YR-1 research have been accomplished. In addition to the research that guaranteed to be accomplished in Phase I, and was, the following additional research was completed or initiated:

- A prototype Fiber Detector was designed, fabricated, and tested in the laboratory and at the Intense Pulsed Neutron Source. The Fiber Detector (FD) has been demonstrated to successfully measure neutron arrivals from an accelerator-based pulsed neutron source; this was not anticipated to be undertaken until about one year into Phase II research.

- The FD is not only Position Sensitive in 1D for individual neutron arrivals, but also in 2D for populations of neutron captures.

- The detector produced in Phase I can be utilized for preliminary testing of 2D sensitivity for individual neutron captures early in Phase II. The "left-hand" side of the detector, 3 neutron glass X and 2 neutron glass Y fiber ribbons, were tested during Phase I.

- System electronics are far ahead of schedule; "double coincidence" electronics have been designed and fabrication of the boards has begun for operating 12 signal inputs in all X-X, Y-Y, and X-Y detector element permutations.

- Valuable lessons have been learned for design issues and testing in pulsed neutron environments.

The capability of the FD to measure scattered neutrons in both 1D and 2D during the initial tests at IPNS is very encouraging. One dimensional position sensitivity of this prototype is a given by use of thin detector elements, in this case the glass fibers. The "X" and "Y" orthogonal orientation of the fiber ribbons provides 1D resolutions in each direction with the resolution determined by the number of fibers, *i.e.* width, of each ribbon. For this prototype, a spatial resolution dimension of 0.5 cm (the fiber ribbon widths) was chosen. However resolutions can be as fine as the width of an individual fiber, *i.e.*, about 100 μm of "active diameter." This ability allowed a 2D PSD to be planned for at the outset of the Phase I research, even though 2D was not a deliverable at this stage. This design was planned to be expanded to test a minimum of two additional mechanisms that could allow for detections, with very fast timing, of individual captures and discern their 2D positions in real time. Two dimensional sensitivity for the FD may be achieved by many means, but crossed fiber types of detectors were selected for testing in Phase II and so were anticipated and incorporated in Phase I designs.

The technical feasibility of producing useful and cost-effective detector systems using the neutron sensitive scintillating glass fiber has been demonstrated. Neutron-gamma discrimination has been achieved. Detector system electronics are well engineered, reliable, and have been designed to expand as the system platform grows. Scaling up the present detector and integrating the three or more new detection systems with the system electronics during Phase II may not be as difficult as anticipated, if these initial tests are indicators of future research results.

Large area, position sensitive detector arrays that utilize neutron glass fibers as the array detection medium are not only feasible, but will likely be most economical solution for providing the large area and other specialized detector array systems that are required for the SNS and other neutron science research centers.

Phase II Research and Development are justified for the Scintillating Neutron Sensitive Scintillating Glass Fiber Detector that was developed and tested in Phase I.